International Symposium
Non-Destructive Testing in Civil Engineering (NDT-CE)

September 15 - 17, 2015, Berlin, Germany

Investigations for the Improvement of the SAFT Imaging Quality of a Large Aperture Ultrasonic System

Klaus MAYER [1], Martin KRAUSE [2], Herbert WIGGENHAUSER [2], Boris MILMANN [2]

[1] Computational Electronics and Photonics, University of Kassel, Kassel, Germany
[2] BAM – Federal Institute for Materials Research and Testing, Berlin, Germany

Abstract
In parallel to the hardware development of an ultrasonic system for the investigation of thick concrete structures, a software package for interactive reconstruction of data for that special arrangement of ultrasonic transducers was developed. The system which is presented in a further contribution to this conference as "large aperture ultrasonic system" (LAUS) requires special features to the evaluation software because measuring positions can be in a non equidistant grid and there is the possibility to improve the measurement by adding measuring points interactively.

Starting from theoretical considerations to the image generation by measuring arrangements of synthetic aperture problems, solution approaches for imaging with SAFT (Synthetic Aperture Focusing Technique) algorithms in space and frequency domain of data from insufficient grid density are presented.

A wide range of issues that may arise in the application is precalculated by simulations and experimental studies, so that unavoidable artifacts can be identified and classified. A special focus is put on the application of thick concrete structures considering missing measuring points in a grid, grating lobes and surface waves.

Keywords: Ultrasound imaging, synthetic aperture focusing technique (SAFT), linear array, grating lobe reduction

1. Introduction

Imaging methods like SAFT (Synthetic Aperture Focusing Technique) have been serving to optimize and to objectify the evaluation of ultrasonic measurements for years. The method reached the application in the field of nondestructive testing of concrete building elements relatively late, because the reproducible insonification and the large area measurement without coupling agent have become possible by new sensor techniques like point contact and air coupled ultrasonic transducers. The broadband impulse like signals gained by these measurement techniques can be evaluated by classical diffraction tomographic algorithms. Specific to the evaluation of data of the Large Aperture Ultrasonic System [1] is on the one hand the radiation characteristic of the single ultrasound unit, which consists of 32 single point contact transducers in a dedicated arrangement and on the other hand the capability of a free positioning of 12 transducer units. The hardware is operated comparable to a smaller handheld unit of the same manufacturer [2] as a linear array, this means that if one of the 12 transducer units is sending, all other units are switched to receive the signals. This is repeated for all 12 transducers, so that finally 12 x 11 measured A-scans can be used for further processing. The algorithm for the image formation is borrowed from the SAFT principle. An image is generated by the fact that each pixel of the image represents a position in space with a distance from the transmitter and from the receiver for any A-scan signal. The travel time

for a wave coming from the transmitter plus the travel time of a wave returning to a receiver is used to select a sampling value in the A-scan signal and to add this value into the pixel memory. This is repeated for all received signals, so that we finally have a delay and sum algorithm for any pixel and for all A-scans. The superposition of the data of all measurement points delivers an intensity image of the reflectivity of ultrasonic scattering centers by constructive and destructive interference. The question remains how the image represents the real scattering geometry and what are the reasons of deviations.

Figure 1: One ultrasonic unit of the LAUS system. Each Module consists of 32 dry point contact transducers which are spring loaded and ensure the mechanical contact to the concrete surface. It is fixed using a vacuum case. Additionally there is a electronic module for data transfer.

2. The ultrasonic transducer unit

The ultrasonic transducer unit consists of an arrangement of point contact transducers (Figure 1). Each single transducer generates an ultrasonic shear wave impulse. Because of reciprocity a transducer used as receiver has the same characteristic. For a detailed analysis a 3D-EFIT simulation (Elastodynamic Finite Integration Technique [3, 4]) of the transducer unit was done to calculate the propagation of an elastic wave in a volume with the material characteristic of concrete. Figure 2 shows the magnitude of the velocity vector for two different time snapshots. The first very early snapshot shows the evolution of small spherical waves, which have their origin at every single tip of the point contact transducers. The later time snapshot shows the development of the wave in space, which has a different behavior in the orthogonal planes because of polarization effects. The xz-plane (marked red) shows the properties of an SV (shear vertical) wave with pressure, head, and Rayleigh surface waves. The yz-plane (marked cyan) shows the behavior of SH (shear horizontal) waves, which are pure shear waves without other wave types and with broad angle radiation characteristic. This ideal behavior is reached only if the source is part of the plane (Figure 2a-e), which is not the case in a second simulation displayed in figure 2f where the recording planes are outside the transducer area-

Figure 3 (top) shows the impulse behavior of the transducer unit on an axial line through the center of the transducer. As excitation wavelet an RC2 (raised cosine with 2 cycles) signal with a center frequency of 50 kHz was used, which comes close to the form of the real signal due to band limitation occurring by resonance properties of the probes. Due to the different distances of the individual probes, it comes to a delayed overlay, which results in a depth-

dependent deformation of the impulse. A phase analysis [5, 6] at the center frequency of the signal at the maximum of the envelope shows a depth-dependent profile (figure 3 bottom) where it comes to a relatively strong deviation in the near field of the transducer.

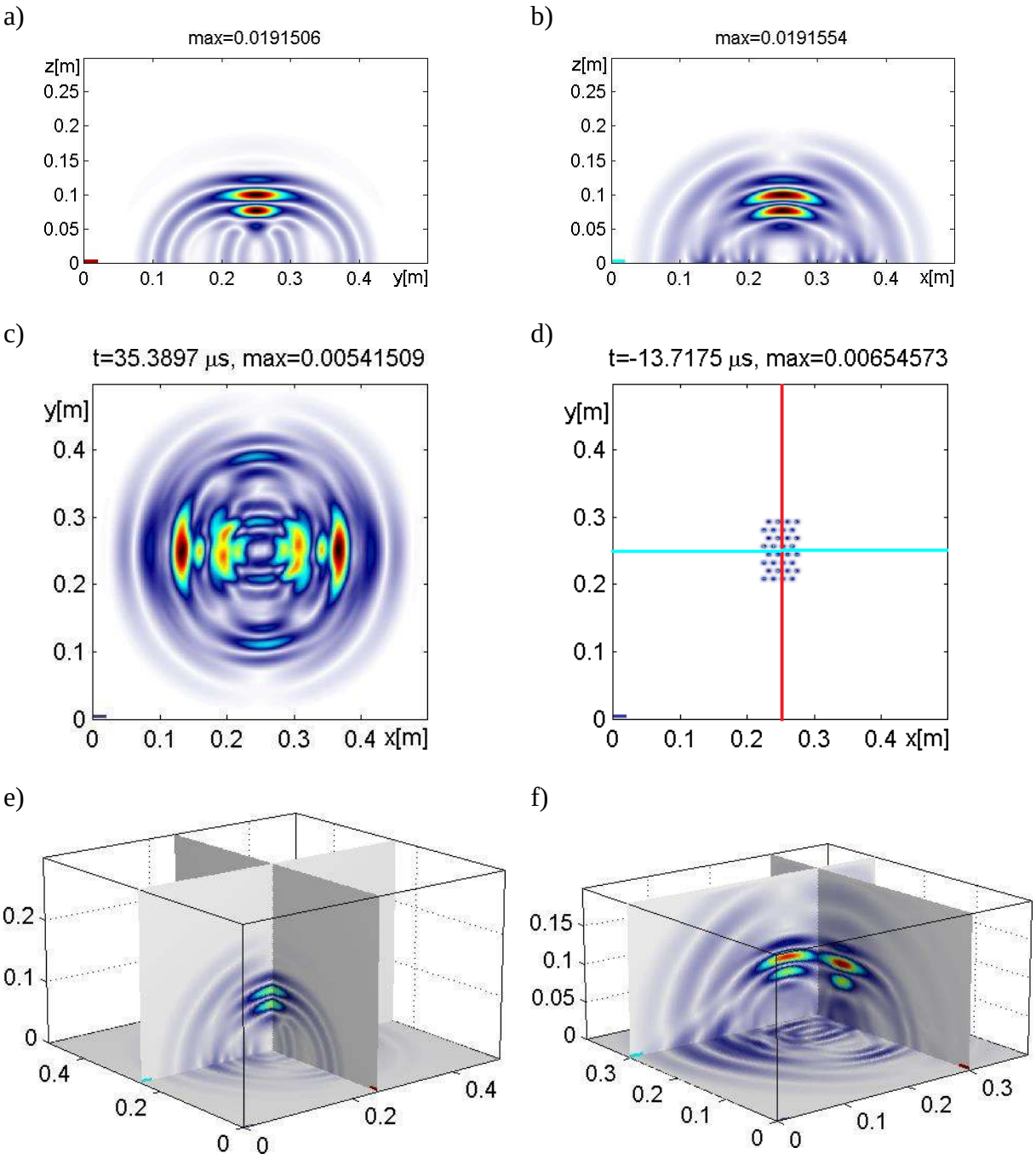

Figure 2: Results of 3D-EFIT simulation of LAUS transducer unit excited into x-direction by a 55 kHz RC2 impulse a) Magnitude of velocity vector in yz-plane at time t = 35µs (SH-wave). b) Velocity vector in zx-plane (SV-wave). c) Velocity vector in the surface (xy-plane). d) Velocity vector in the surface at very early time, shown the location of the section planes. e) Common display of all three planes in the volume. f) Display of all planes near to the border of the transducer (Result from a different simulation, with CPML [7] boundary condition and transducer not in the center of the surface).

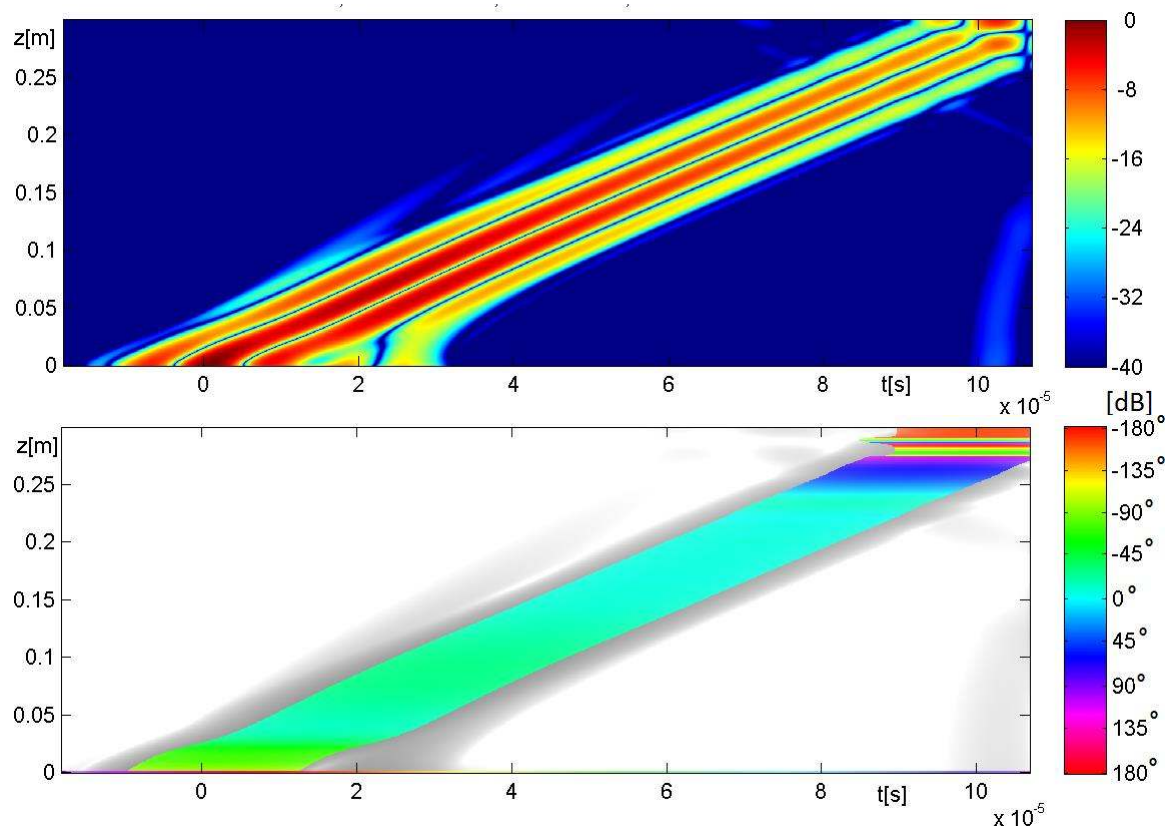

Figure 3: 3D-EFIT Simulation: amplitude (top) and phase values (bottom) of the velocity vector along a central line under the transducer unit. Phase values for depth: 0.01m: -79°, 0.05m: -18°, 0.1m: -28°, 0.15m: -10°, 0.2m: -9°. The strong deviation in the depth of 0.25 m are caused by the superposition with the back wall echo.

3. The reconstruction algorithm for the linear array system

Based on the SAFT algorithm a travel time corrected superposition of all A-scans is performed. The manufacturer already provides a software with such a technique. For systematic evaluation and taking different conditions into account a software package with the name InterSAFT [8] was developed which stands for interactive handling of 2D- and 3D-SAFT applications. As result of a SAFT reconstruction an image with location accuracy and contour sharpness of the given arrangement of scattering centers, which means the arrangement of ultrasonic reflecting objects in a homogeneous background material can be expected so that a trained user can draw conclusions about his current problem.

The question why the superposition of delayed single measurements delivers an image and what this image means can only be answered by a mathematical treatment of the problem.

The measurement is the recording of many individual events but finally it is a recording of wave phenomena resulting from some single shot experiments. A monostatic measurement can be combined to a single and unique integral equation, which can be solved by diffraction tomography for the unknown scattering object with well known linearizing approximations like the born or physical optics approximations [9, 10]. The linear array measurement however is not monostatic, i.e. the recorded signal is not generated by a transmitted signal on the same (or very nearby) sending point, but the signal is connected to multiple receiving

points. So, the idea behind SAFT may be transferred to a linear array arrangement, but this is not covered by the mathematical theory of SAFT. If we consider diffraction tomography algorithms more in detail [11], we see, that they consist of the idea to back propagate the received wave field to the sources, where they were generated. In the linear array case, the primary source of each wave field is a point source at the surface which illuminates the scattering object, which is the 'secondary' source for the received wave field. It follows, that we have to back propagate the wave field to a point in the reconstruction area, but we have to stop the back propagation at the time when the source field reaches that point. This time is different for each pixel in the reconstruction. Since the secondary source is not only illuminated by the primary source, but also by multiple reflections of the wave field of the primary source, a further idea is to superimpose all interactions of the primary wave field with the scattering object, which gives us the RTM (reverse time migration) algorithm [12]. The advantage of that method is, that we get information from illuminations of the scattering object from different directions and we can incorporate prior information to the reconstruction process.

From diffraction tomography we know, that a reconstruction - the image - is the Fourier back-transform of a spectral image, the so called K-space. The sharpness of an image depends of the bandwidth of its spectrum. But this says nothing about the quality of the reconstruction. For imaging algorithms one uses the PSF (point spread function), which shows the imaging quality of the smallest element of a reconstruction - a point-like reflector. For imaging algorithms the PSF is not space invariant, it depends on the distance to the measurement surface and on the lateral position under the surface, because the measurement area is usually limited in size.

Solving the integral equation of diffraction tomography means to back-propagate the wave field at the surface back to the sources [13]. With this knowledge we have recognized that SAFT itself is a wave propagation algorithm and therefore SAFT underlies the same diffraction effects like e.g. antenna arrays [14]. This means, we find side lobes - caused by aperture apodisation - but also grating lobes characterized by the finite number of single transducer units which have a finite distance to each other. The PSF shows side lobes as cross-shaped expansions, which centers are located at the end of the aperture. Whereas grating lobes manifest themselves as extended side maxima in larger distances of the center of the PSF. The focusing effect results from uniform superposition of waves propagating from all receiving positions. A non-uniform antenna configuration for antenna arrays can be used to suppress distinct directions from the antenna beam. Applied to imaging algorithms, this leads however to unpredictable deformations of the PSF.

3.1. Optimization of data processing by replacing missing information.

Figure 4 (left) shows the simulated reflection data of a point-like scatterer in a depth of 1m. Displayed are 132 A-scans, which can be received if 12 transmitter units interact with 11 receiver units respectively. It is noticeable, that for each sending position there is a discontinuity in the signal locus curve which results from the fact, that a transmitter cannot be a receiver at the same time. The full reconstruction is a superposition of all single

reconstructions, which was calculated by a single sending position. This means, that if there is an inconsistency in a single reconstruction, this will be visible in the full reconstruction.

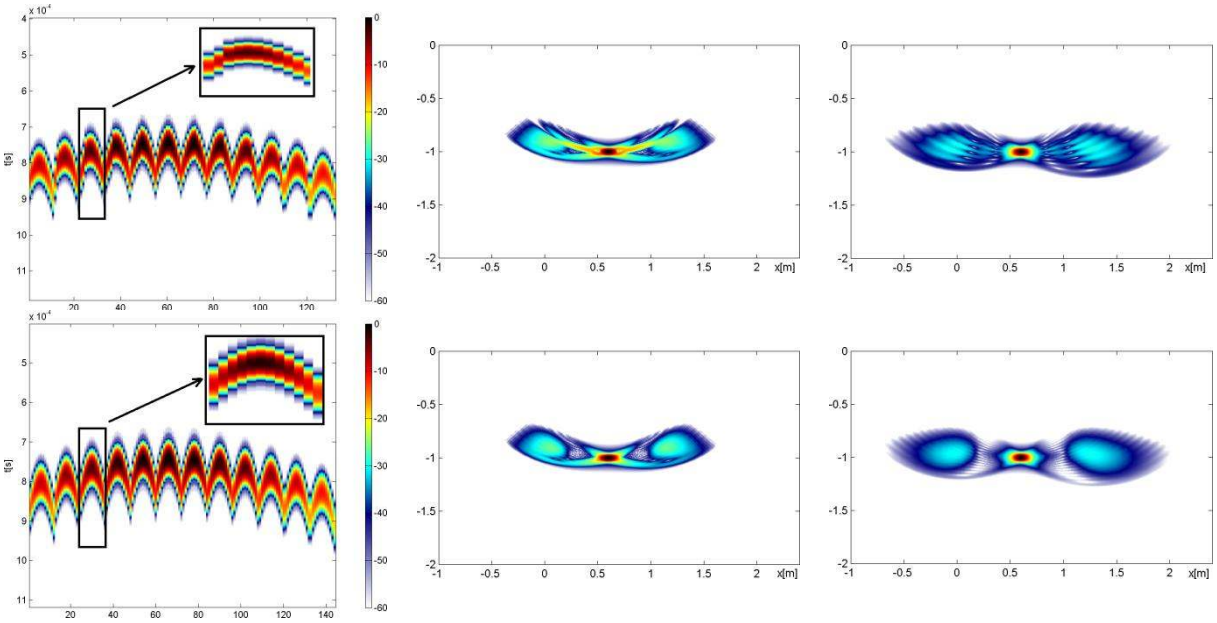

Figure 4: Data and reconstruction of a simulated point-like scatterer in a LAUS arrangement. Depth: 1m. Left: Data of all A-Scans. Mid: Reconstruction of the data of the single transmitting transducer no. 6. Right: Reconstruction of all data. Top: Data with missing monostatic receiver. Bottom: Data replaced by neighboring events.

By a simple trick we can solve the problem of the missing receiving point. Instead of a monostatic measurement point, we use a bistatic measurement point, which represents the same area of information. Example: We miss the receiving point at position 3: (R3) for the sending position 3: (S3). We replace it by the measurement point 4: (R4), generated by the sending position 2: (S2). Thus, the information from the same area is present without any interpolation, because these A-scans are available in the whole measurement. As there is no replacement for the constellation (S1,R1) and (S12,R12) it is useful not to use a replacement for these measurement points. Figure 4 (bottom) shows the data with inserted A-scans. In comparison to figure 4 (top) we see, that the reconstruction is much smoother and the area around the scatterer is free from artifacts far more than the dynamic range of 60dB can resolve.

3.2. Suppressing of grating lobe effects

Grating lobes known from the application of linear antennas cause ambiguous artifacts for imaging processes. But these artifacts are always associated with the respective main indication. If there are more reflectors in an area, smaller indications may be outshined by the grating lobes of a bigger indication. The grating lobe artifacts cannot be suppressed during the SAFT process. The information available in the data appears exactly where it must appear because the information is not better specified by the fact of undersampling. The additional information which we use here is the fact that a grating lobe effect appears only if the respective main indication is available. Therefore the idea must be to eliminate all contributions of the main indication from the measurement data, then the depending grating

lobes will also disappear. The processing is as follows: a) Take a complete dataset from measurement. b) Reconstruct the data. c) Search large scattering centers and cut these out of the reconstruction. d) Generate synthetic measurement data of the original reconstruction and of the cleanly cut large scattering centers by wave propagation. e) Subtract both synthetic data from each other to get data for smaller scatterers only. f) Reconstruct again the difference data.

Figure 5 shows the result of the method for two synthetic scatterers which differ in reflection intensity by 20dB.

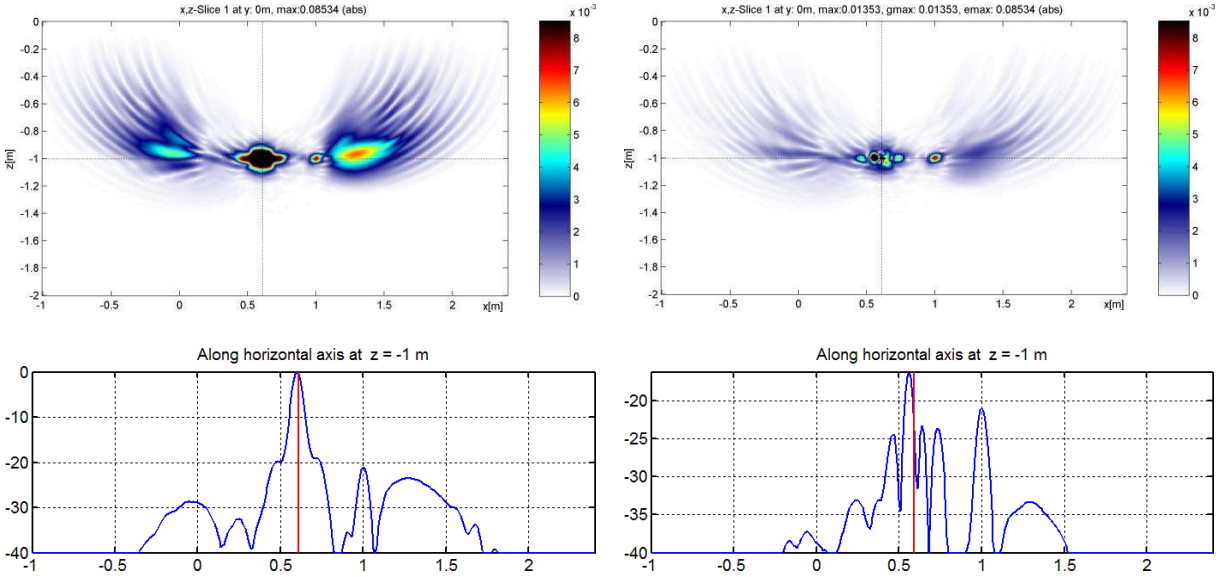

Figure 5: Reconstruction of two synthetic point like scatterers with 20dB difference in amplitude. Left: Original SAFT image. Right: Result of processing to suppress main scatterer grating lobes. Top: SAFT image with amplitude limited to the intensity of the small scatterer. Bottom: Amplitude along a line at z=-1m in logarithmic scale.

3.3 Optimization of grating lobe effects by surface wave suppression.

As already mentioned, grating lobe effects appear if there are strong scattering events in the data. These grating lobes effects appear even if the strong events are not in the area of interest, or in the area of reconstruction. Therefore reflection of edges or corners from the limits of the object appear in the data and may be far away from the area of interest. The method above is not so suitable for that problem, because the reflected waves travel with different velocities and are not well focused in the SAFT image. A separate preprocessing module has been developed to detect and to interactively suppress surface waves with different velocities and from different borders. Figure 6 shows the measurement setup from a large concrete block at BAM, where LAUS data have been acquired. Figure 7 shows the reconstruction before surface waves suppression (left) and after surface waves suppression (right). In the indicated area (B) a significant grating lobe reduction can be observed which results from strong reflection from the corners of the specimen (A). The indications of the corners are not at the correct place (and would normally not be displayed) because they appear outside of the specimen. The surface waves suppressed in this example travel with a velocity of 2600m/s, whereas the velocity of concrete for SAFT imaging was assumed to be 2700m/s.

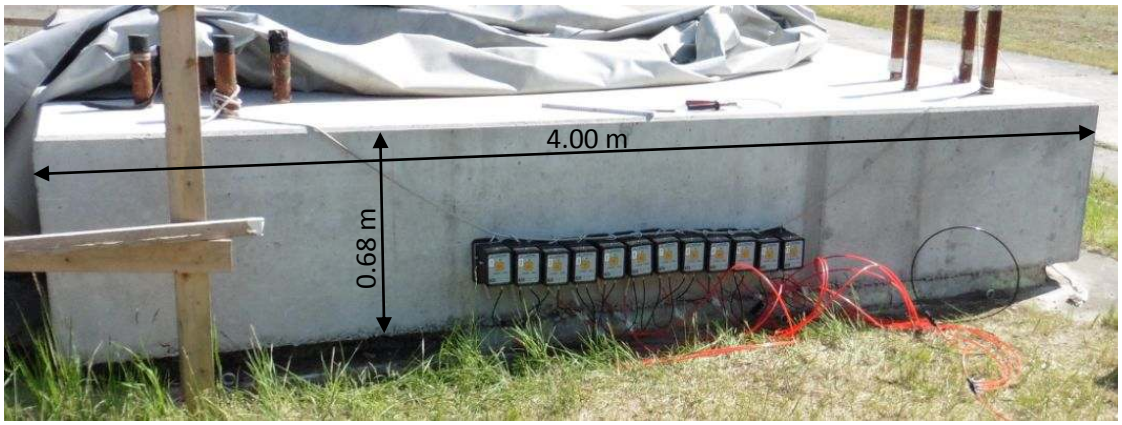

Figure 6: LAUS mounted at foundation slab imaging the back wall echo (4 m) and internal reflectors as presented in figure 7

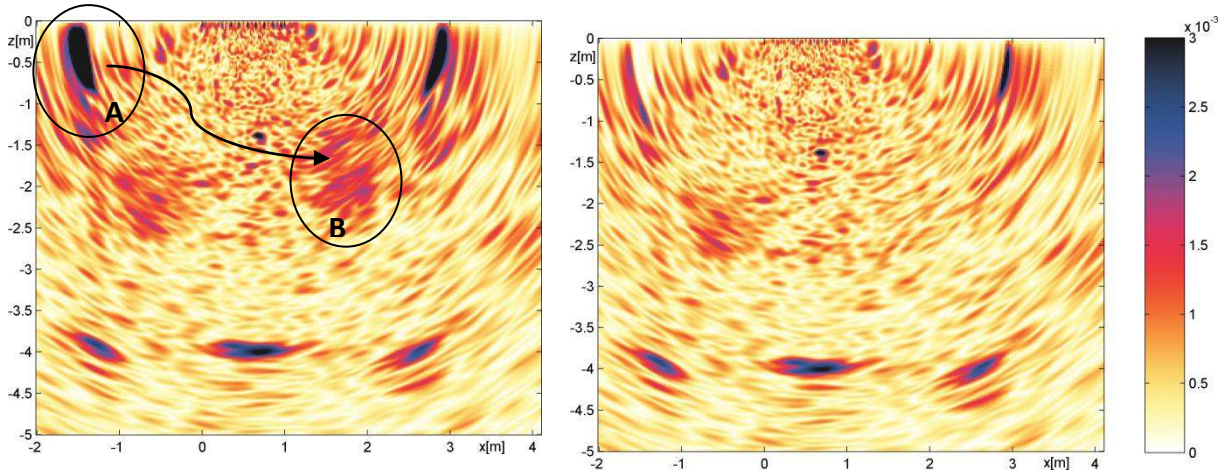

Figure 7: LAUS imaging results on a large foundation slab of 4m x 4m and 0.680m thickness. LAUS was mounted on one front side of the slab. Left: SAFT without surface wave suppression. Right: SAFT with surface wave suppressed by preprocessing

4. Conclusion

With the Large Aperture Ultrasonic System measurement capabilities were reached which opens a promising door for future ultrasonic inspection of large concrete components. With the hardware capabilities and the flexibility of mounting and usage of the single devices many aspects of array imaging can be applied and have to be elaborated for many different imaging scenarios. Some aspects like side lobe and grating lobe suppression have been discussed here but the wide area of SAFT imaging with data acquired at a non equidistant grid is still a future and exciting research topic.

References

1. H. Wiggenhauser, A. Samokrutov, K. Mayer, M. Krause, S. Alekhin, V. Elkin, 'LAUS – Large Aperture Ultrasonic System – for Testing Thick Concrete Structures'. ASCE Journal of Infrastructure systems, submitted
2. A. V. Bishko, A. A. Samokrutov, V. G. Shevaldykin, 'Ultrasonic echopulse tomography of concrete using shear waves low frequency phased antenna arrays'. Proc. 17th World Conference on Nondestructive Testing, Shanghai, China. (2008)
3. R. Marklein, 'The finite integration technique as a general tool to compute acoustic, electromagnetic, elastodynamic and coupled wave fields'. In: Stone WR, editor. Review of radio science 1999–2002. Piscataway: IEEE Press; (2002)
4. P. Fellinger, R. Marklein, K. J. Langenberg, S. Klaholz, 'Numerical modeling of elastic wave propagation and scattering with EFIT—elastodynamic finite integration technique'. Wave motion , 21(1), 4766, (1995)
5. K. Mayer, K. J. Langenberg, M. Krause, B. Milmann, F. Mielentz, 'Characterization of Reflector Types by Phase-Sensitive Ultrasonic Data Processing and Imaging'. J Nondestruct Eval 27, 35–45, (2008)
6. S. Schulze, M. Krause, K Mayer, B. Redmer, H. Wiggenhauser, 'Grouting Defects Localized by Ultrasonic Testing Including Phase Evaluation'. Proc., ASNT Topical Conference, NDE/NDT for Highways and Bridges, Structural Materials Technology (SMT) , Washington, DC, USA, 321328 (2014)
7. P. K. Chinta, K. Mayer, K. J. Langenberg, J. Prager, J., 2012. 'Three-Dimensional Elastic Wave Modeling in Austenitic Steel Welds using Elastodynamic Finite Integration Technique'. In: 18the World Conference on Nondestructive Testing. Durban (2012)
8. K. Mayer, P. K. Chinta: InterSAFT Software for interactive SAFT processing of ultrasound and Radar data. Developed at the department of computational electronics and photonics, University of Kassel (2008 – 2014)
9. K. J. Langenberg, R. Marklein, K. Mayer, 'Ultrasonic Nondestructive Testing of Materials: Theoretical Foundations'. CRC Press Inc, Boca Raton. (2012)
10. K. J. Langenberg, K. Mayer, R. Marklein, 'Nondestructive testing of concrete with electromagnetic and elastic waves: Modeling and imaging'. Cement & Concrete Composites, Vol. 28, No. 4, pp. 370-383 (2006)
11. A. J. Devaney, 'Geophysical Diffraction Tomography'. IEEE Transactions on Geoscience and Remote Sensing GE-22, 3–13. (1984)
12. E. Baysal, D. D. Kosloff, J. W. C. Sherwood: 'Reverse time migration'. Geophysics vol. 48, no. II (November 1983); P. 1514-1524,
13. K. Mayer, P. K. Chinta, K. J. Langenberg, M. Krause, 'Ultrasonic Imaging of Defects in Known Anisotropic and Inhomogeneous Structures with Fast Synthetic Aperture Methods'. Presented at the WCNDT 2012, Durban. (2012)
14. C.A. Balanis, Antenna Theory, w. CDROM: Analysis and Design , Wiley & Sons, New York. (1996)